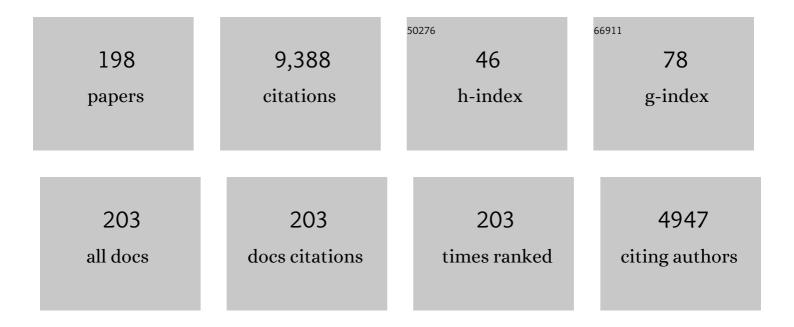
## Joseph Carroll

List of Publications by Year in descending order

Source: https://exaly.com/author-pdf/6530235/publications.pdf Version: 2024-02-01



LOSEDH CADDOLL

#	Article	IF	CITATIONS
1	Long-term retinal imaging of a case of suspected congenital rubella infection. American Journal of Ophthalmology Case Reports, 2022, 25, 101241.	0.7	3
2	Pupillary Dilation in Research: More than Meets the Eye. Current Eye Research, 2022, , 1-13.	1.5	0
3	Comparison of Cone Mosaic Metrics From Images Acquired With the SPECTRALIS High Magnification Module and Adaptive Optics Scanning Light Ophthalmoscopy. Translational Vision Science and Technology, 2022, 11, 19.	2.2	5
4	Axial Length Distributions in Patients With Genetically Confirmed Inherited Retinal Diseases. , 2022, 63, 15.		6
5	Promises and pitfalls of evaluating photoreceptor-based retinal disease with adaptive optics scanning light ophthalmoscopy (AOSLO). Progress in Retinal and Eye Research, 2021, 83, 100920.	15.5	29
6	Characterizing Current Attitudes and Practices for Human Subject Safety in Studies Involving Pupil Dilation. Journal of Empirical Research on Human Research Ethics, 2021, 16, 54-64.	1.3	1
7	Color vision. Handbook of Clinical Neurology / Edited By P J Vinken and G W Bruyn, 2021, 178, 131-153.	1.8	7
8	Optical Coherence Tomography Artifacts Are Associated With Adaptive Optics Scanning Light Ophthalmoscopy Success in Achromatopsia. Translational Vision Science and Technology, 2021, 10, 11.	2.2	8
9	Comparison of confocal and non-confocal split-detection cone photoreceptor imaging. Biomedical Optics Express, 2021, 12, 737.	2.9	13
10	Examining Whether AOSLO-Based Foveal Cone Metrics in Achromatopsia and Albinism Are Representative of Foveal Cone Structure. Translational Vision Science and Technology, 2021, 10, 22.	2.2	5
11	Aberrant visual population receptive fields in human albinism. Journal of Vision, 2021, 21, 19.	0.3	4
12	Automated image processing pipeline for adaptive optics scanning light ophthalmoscopy. Biomedical Optics Express, 2021, 12, 3142.	2.9	5
13	Optical Coherence Tomography Angiography in the Thirteen-Lined Ground Squirrel. Translational Vision Science and Technology, 2021, 10, 5.	2.2	0
14	Cone photoreceptor reflectance variation in the northern tree shrew and thirteen-lined ground squirrel. Experimental Biology and Medicine, 2021, 246, 2192-2201.	2.4	3
15	Pathognomonic macular ripples are revealed by polarized infrared retinal imaging. Experimental Biology and Medicine, 2021, 246, 2202-2206.	2.4	2
16	Comparing Retinal Structure in Patients with Achromatopsia and Blue Cone Monochromacy Using OCT. Ophthalmology Science, 2021, 1, 100047.	2.5	4
17	Theoretical versus empirical measures of retinal magnification for scaling AOSLO images. Journal of the Optical Society of America A: Optics and Image Science, and Vision, 2021, 38, 1400.	1.5	2
18	Retinal alterations in patients with Lafora disease. American Journal of Ophthalmology Case Reports, 2021, 23, 101146.	0.7	4

#	Article	IF	CITATIONS
19	Pre-retinal delivery of recombinant adeno-associated virus vector significantly improves retinal transduction efficiency. Molecular Therapy - Methods and Clinical Development, 2021, 22, 96-106.	4.1	0
20	ATF6 is essential for human cone photoreceptor development. Proceedings of the National Academy of Sciences of the United States of America, 2021, 118, .	7.1	31
21	Challenges Associated With Ellipsoid Zone Intensity Measurements Using Optical Coherence Tomography. Translational Vision Science and Technology, 2021, 10, 27.	2.2	15
22	Assessing Foveal Structure in Individuals with TYR R402Q and S192Y Hypomorphic Alleles. Ophthalmology Science, 2021, 1, 100077.	2.5	2
23	Foveal avascular zone morphology and parafoveal capillary perfusion in sickle cell retinopathy. British Journal of Ophthalmology, 2020, 104, 473-479.	3.9	15
24	Assessing the Use of Incorrectly Scaled Optical Coherence Tomography Angiography Images in Peer-Reviewed Studies. JAMA Ophthalmology, 2020, 138, 86.	2.5	70
25	Visual Acuity and Foveal Structure in Eyes with Fragmented Foveal Avascular Zones. Ophthalmology Retina, 2020, 4, 535-544.	2.4	11
26	Noninvasive Imaging of Cone Ablation and Regeneration in Zebrafish. Translational Vision Science and Technology, 2020, 9, 18.	2.2	5
27	Assessing the Influence of OCT-A Device and Scan Size on Retinal Vascular Metrics. Translational Vision Science and Technology, 2020, 9, 7.	2.2	12
28	Photobiomodulation preserves mitochondrial redox state and is retinoprotective in a rodent model of retinitis pigmentosa. Scientific Reports, 2020, 10, 20382.	3.3	16
29	On the axial location of Gunn's dots. American Journal of Ophthalmology Case Reports, 2020, 19, 100757.	0.7	8
30	Intraobserver Repeatability and Interobserver Reproducibility of Foveal Cone Density Measurements in <i>CNGA3-</i> and <i>CNGB3</i> -Associated Achromatopsia. Translational Vision Science and Technology, 2020, 9, 37.	2.2	10
31	Long-Term Investigation of Retinal Function in Patients with Achromatopsia. , 2020, 61, 38.		19
32	The relationship between retinal cone density and cortical magnification in human albinism. Journal of Vision, 2020, 20, 10.	0.3	8
33	Preservation of the Foveal Avascular Zone in Achromatopsia Despite the Absence of a Fully Formed Pit. , 2020, 61, 52.		7
34	Seeking clarity on retinal findings in patients with COVID-19. Lancet, The, 2020, 396, e38.	13.7	14
35	Assessing Interocular Symmetry of the Foveal Cone Mosaic. , 2020, 61, 23.		14
36	Comparison of the Morphology of the Foveal Pit Between African and Caucasian Populations. Translational Vision Science and Technology, 2020, 9, 24.	2.2	13

#	Article	IF	CITATIONS
37	Electroretinogram of the Cone-Dominant Thirteen-Lined Ground Squirrel during Euthermia and Hibernation in Comparison with the Rod-Dominant Brown Norway Rat. , 2020, 61, 6.		7
38	Interocular asymmetry of foveal avascular zone morphology and parafoveal capillary density in sickle cell retinopathy. PLoS ONE, 2020, 15, e0234151.	2.5	2
39	Assessing Ganglion Cell Layer Topography in Human Albinism Using Optical Coherence Tomography. , 2020, 61, 36.		15
40	Photoreceptor Structure in <i>GNAT2 </i> -Associated Achromatopsia. , 2020, 61, 40.		25
41	Longitudinal Assessment of Remnant Foveal Cone Structure in a Case Series of Early Macular Telangiectasia Type 2. Translational Vision Science and Technology, 2020, 9, 27.	2.2	8
42	Interocular Symmetry of Foveal Cone Topography in Congenital Achromatopsia. Current Eye Research, 2020, 45, 1257-1264.	1.5	23
43	Baseline Visual Field Findings in the RUSH2A Study: Associated Factors and Correlation With Other Measures of Disease Severity. American Journal of Ophthalmology, 2020, 219, 87-100.	3.3	22
44	Multiexon deletion alleles of ATF6 linked to achromatopsia. JCl Insight, 2020, 5, .	5.0	13
45	Characterization of Retinal Structure in <i>ATF6</i> -Associated Achromatopsia. , 2019, 60, 2631.		43
46	Novel Development of Parafoveal Capillary Density Deviation Mapping using an Age-Group and Eccentricity Matched Normative OCT Angiography Database. Translational Vision Science and Technology, 2019, 8, 1.	2.2	14
47	Assessing Retinal Structure in Patients with Parkinson Disease. Journal of Neurology & Neurophysiology, 2019, 10, .	0.1	6
48	Interocular symmetry, intraobserver repeatability, and interobserver reliability of cone density measurements in the 13-lined ground squirrel. PLoS ONE, 2019, 14, e0223110.	2.5	2
49	Earliest Evidence of Preclinical Diabetic Retinopathy Revealed Using Optical Coherence Tomography Angiography Perfused Capillary Density. American Journal of Ophthalmology, 2019, 203, 103-115.	3.3	112
50	The Utility of Frame Averaging for Automated Algorithms in Analyzing Retinal Vascular Biomarkers in AngioVue OCTA. Translational Vision Science and Technology, 2019, 8, 10.	2.2	17
51	Noninvasive imaging of the tree shrew eye: Wavefront analysis and retinal imaging with correlative histology. Experimental Eye Research, 2019, 185, 107683.	2.6	34
52	Evaluating seasonal changes of cone photoreceptor structure in the 13-lined ground squirrel. Vision Research, 2019, 158, 90-99.	1.4	21
53	Adaptive Optics Retinal Imaging in <i>CNGA3</i> -Associated Achromatopsia: Retinal Characterization, Interocular Symmetry, and Intrafamilial Variability. , 2019, 60, 383.		43
54	Assessing the Interocular Symmetry of Foveal Outer Nuclear Layer Thickness in Achromatopsia. Translational Vision Science and Technology, 2019, 8, 21.	2.2	18

#	Article	IF	CITATIONS
55	Noninvasive Imaging and Correlative Histology of Cone Photoreceptor Structure in the Pig Retina. Translational Vision Science and Technology, 2019, 8, 38.	2.2	11
56	Deep Phenotyping of <i>PDE6C</i> -Associated Achromatopsia. , 2019, 60, 5112.		44
57	Acid Ceramidase Deficiency in Mice Leads to Severe Ocular Pathology and Visual Impairment. American Journal of Pathology, 2019, 189, 320-338.	3.8	16
58	CELLULAR IMAGING OF THE TAPETAL-LIKE REFLEX IN CARRIERS OF RPGR-ASSOCIATED RETINOPATHY. Retina, 2019, 39, 570-580.	1.7	25
59	RAC-CNN: multimodal deep learning based automatic detection and classification of rod and cone photoreceptors in adaptive optics scanning light ophthalmoscope images. Biomedical Optics Express, 2019, 10, 3815.	2.9	30
60	Evaluating relationships between cone density, ganglion cell metrics, and foveal structure. Journal of Vision, 2019, 19, 17.	0.3	0
61	Advances in Imaging-Based Biomarkers for Studying Retinal Disease. Journal of Vision, 2019, 19, 23.	0.3	1
62	A Natural Experiment in Aberrant Retino-Cortical Organization. Journal of Vision, 2019, 19, 212b.	0.3	0
63	Foveal Development in Infants Treated with Bevacizumab or Laser Photocoagulation for Retinopathy of Prematurity. Ophthalmology, 2018, 125, 444-452.	5.2	38
64	Adaptive optics imaging of inherited retinal diseases. British Journal of Ophthalmology, 2018, 102, 1028-1035.	3.9	61
65	Imaging retinal melanin: a review of current technologies. Journal of Biological Engineering, 2018, 12, 29.	4.7	50
66	Assessing photoreceptor structure in patients with traumatic head injury. BMJ Open Ophthalmology, 2018, 3, e000104.	1.6	7
67	The Henle Fiber Layer in Albinism: Comparison to Normal and Relationship to Outer Nuclear Layer Thickness and Foveal Cone Density. , 2018, 59, 5336.		26
68	Axial Scaling Is Independent of Ocular Magnification in OCT Images. , 2018, 59, 3037.		14
69	Longitudinal Assessment of Retinal Structure in Achromatopsia Patients With Long-Term Follow-up. , 2018, 59, 5735.		39
70	Variability of Foveal Avascular Zone Metrics Derived From Optical Coherence Tomography Angiography Images. Translational Vision Science and Technology, 2018, 7, 20.	2.2	42
71	Intraobserver Repeatability and Interobserver Reproducibility of Ellipsoid Zone Measurements in Retinitis Pigmentosa. Translational Vision Science and Technology, 2018, 7, 13.	2.2	10
72	lmaging Melanin Distribution in the Zebrafish Retina Using Photothermal Optical Coherence Tomography. Translational Vision Science and Technology, 2018, 7, 4.	2.2	32

#	Article	IF	CITATIONS
73	Deep learning based detection of cone photoreceptors with multimodal adaptive optics scanning light ophthalmoscope images of achromatopsia. Biomedical Optics Express, 2018, 9, 3740.	2.9	41
74	Residual Cone Structure in Patients With X-Linked Cone Opsin Mutations. , 2018, 59, 4238.		29
75	Fast adaptive optics scanning light ophthalmoscope retinal montaging. Biomedical Optics Express, 2018, 9, 4317.	2.9	23
76	Assessment of Outer Retinal Remodeling in the Hibernating 13-Lined Ground Squirrel. , 2018, 59, 2538.		23
77	Automatic Cone Photoreceptor Localisation in Healthy and Stargardt Afflicted Retinas Using Deep Learning. Scientific Reports, 2018, 8, 7911.	3.3	49
78	Parafoveal Nonperfusion Analysis in Diabetic Retinopathy Using Optical Coherence Tomography Angiography. Translational Vision Science and Technology, 2018, 7, 4.	2.2	44
79	Reply. Ophthalmology, 2018, 125, e57.	5.2	0
80	Repeatability and Reproducibility of In Vivo Cone Density Measurements in the Adult Zebrafish Retina. Advances in Experimental Medicine and Biology, 2018, 1074, 151-156.	1.6	4
81	A method for age-matched OCT angiography deviation mapping in the assessment of disease- related changes to the radial peripapillary capillaries. PLoS ONE, 2018, 13, e0197062.	2.5	27
82	Within-subject assessment of foveal avascular zone enlargement in different stages of diabetic retinopathy using en face OCT reflectance and OCT angiography. Biomedical Optics Express, 2018, 9, 5982.	2.9	29
83	Aberrant Population Receptive Fields in Albinism. Journal of Vision, 2018, 18, 204.	0.3	0
84	Assessing the spatial relationship between fixation and foveal specializations. Vision Research, 2017, 132, 53-61.	1.4	49
85	Vision science and adaptive optics, the state of the field. Vision Research, 2017, 132, 3-33.	1.4	115
86	PHOTORECEPTOR INNER SEGMENT MORPHOLOGY IN BEST VITELLIFORM MACULAR DYSTROPHY. Retina, 2017, 37, 741-748.	1.7	33
87	Evaluating outer segment length as a surrogate measure of peak foveal cone density. Vision Research, 2017, 130, 57-66.	1.4	54
88	Quantitative Analysis of Retinal Structure Using Spectral-Domain Optical Coherence Tomography in RPGR -Associated Retinopathy. American Journal of Ophthalmology, 2017, 178, 18-26.	3.3	30
89	Photoreceptor disruption and vision loss associated with central serous retinopathy. American Journal of Ophthalmology Case Reports, 2017, 8, 74-77.	0.7	6
90	A case of congenital retinal macrovessel in an otherwise normal eye. American Journal of Ophthalmology Case Reports, 2017, 8, 18-21.	0.7	10

#	Article	IF	CITATIONS
91	Open source software for automatic detection of cone photoreceptors in adaptive optics ophthalmoscopy using convolutional neural networks. Scientific Reports, 2017, 7, 6620.	3.3	65
92	INTRAOPERATIVE IMAGING OF RETAINED PERFLUOROCARBON LIQUID USING SPECTRAL DOMAIN OPTICAL COHERENCE TOMOGRAPHY. Retinal Cases and Brief Reports, 2017, Publish Ahead of Print, 381-384.	0.6	3
93	REPEATABILITY AND LONGITUDINAL ASSESSMENT OF FOVEAL CONE STRUCTURE IN CNGB3-ASSOCIATED ACHROMATOPSIA. Retina, 2017, 37, 1956-1966.	1.7	50
94	Unsupervised identification of cone photoreceptors in non-confocal adaptive optics scanning light ophthalmoscope images. Biomedical Optics Express, 2017, 8, 3081.	2.9	27
95	Assessing the Accuracy of Foveal Avascular Zone Measurements Using Optical Coherence Tomography Angiography: Segmentation and Scaling. Translational Vision Science and Technology, 2017, 6, 16.	2.2	102
96	Photoreceptor-Based Biomarkers in AOSLO Retinal Imaging. , 2017, 58, BIO255.		38
97	Visualization of Radial Peripapillary Capillaries Using Optical Coherence Tomography Angiography: The Effect of Image Averaging. PLoS ONE, 2017, 12, e0169385.	2.5	59
98	High-Resolution Imaging of Intraretinal Structures in Active and Resolved Central Serous Chorioretinopathy. , 2017, 58, 42.		20
99	An Automated Reference Frame Selection (ARFS) Algorithm for Cone Imaging with Adaptive Optics Scanning Light Ophthalmoscopy. Translational Vision Science and Technology, 2017, 6, 9.	2.2	55
100	The Effect of Retinal Melanin on Optical Coherence Tomography Images. Translational Vision Science and Technology, 2017, 6, 8.	2.2	32
101	Reliability and Repeatability of Cone Density Measurements in Patients With Stargardt Disease and <i>RPGR</i> -Associated Retinopathy. , 2017, 58, 3608.		36
102	Cortical Correlates of Aberrant Vernier Acuity in Albinism. Journal of Vision, 2017, 17, 790.	0.3	0
103	Correlating Photoreceptor Mosaic Structure to Clinical Findings in Stargardt Disease. Translational Vision Science and Technology, 2016, 5, 6.	2.2	27
104	Clinical Characteristics, Mutation Spectrum, and Prevalence of Ãland Eye Disease/Incomplete Congenital Stationary Night Blindness in Denmark. , 2016, 57, 6861.		25
105	Evaluating Descriptive Metrics of the Human Cone Mosaic. , 2016, 57, 2992.		91
106	Assessing Photoreceptor Structure in Retinitis Pigmentosa and Usher Syndrome. , 2016, 57, 2428.		81
107	Imaging Foveal Microvasculature: Optical Coherence Tomography Angiography Versus Adaptive Optics Scanning Light Ophthalmoscope Fluorescein Angiography. , 2016, 57, OCT130.		95
108	Effects of Intraframe Distortion on Measures of Cone Mosaic Geometry from Adaptive Optics Scanning Light Ophthalmoscopy. Translational Vision Science and Technology, 2016, 5, 10.	2.2	33

#	Article	IF	CITATIONS
109	Multimodal Imaging of Photoreceptor Structure in Choroideremia. PLoS ONE, 2016, 11, e0167526.	2.5	56
110	Residual Foveal Cone Structure in <i>CNGB3</i> -Associated Achromatopsia. , 2016, 57, 3984.		90
111	Cone Photoreceptor Structure in Patients With X-Linked Cone Dysfunction and Red-Green Color Vision Deficiency. , 2016, 57, 3853.		36
112	ASSESSING PHOTORECEPTOR STRUCTURE ASSOCIATED WITH ELLIPSOID ZONE DISRUPTIONS VISUALIZED WITH OPTICAL COHERENCE TOMOGRAPHY. Retina, 2016, 36, 91-103.	1.7	72
113	Imaging the adult zebrafish cone mosaic using optical coherence tomography. Visual Neuroscience, 2016, 33, E011.	1.0	14
114	Methods for investigating the local spatial anisotropy and the preferred orientation of cones in adaptive optics retinal images. Visual Neuroscience, 2016, 33, E005.	1.0	12
115	Automatic detection of cone photoreceptors in split detector adaptive optics scanning light ophthalmoscope images. Biomedical Optics Express, 2016, 7, 2036.	2.9	55
116	An analytical model of the influence of cone sensitivity and numerosity on the Rayleigh match. Journal of the Optical Society of America A: Optics and Image Science, and Vision, 2016, 33, A228.	1.5	3
117	The cone dysfunction syndromes: TableÂ1. British Journal of Ophthalmology, 2016, 100, 115-121.	3.9	170
118	Reliability and Repeatability of Cone Density Measurements in Patients with Congenital Achromatopsia. Advances in Experimental Medicine and Biology, 2016, 854, 277-283.	1.6	39
119	Multimodal Imaging of the Tapetal-like Reflex in Carriers of RPGR-associated Retinopathy. Journal of Vision, 2016, 16, 15.	0.3	0
120	Retinal Architecture in  RGS9- and  R9AP-Associated Retinal Dysfunction (Bradyopsia). American Journal of Ophthalmology, 2015, 160, 1269-1275.e1.	3.3	15
121	DIRECTIONAL OPTICAL COHERENCE TOMOGRAPHY PROVIDES ACCURATE OUTER NUCLEAR LAYER AND HENLE FIBER LAYER MEASUREMENTS. Retina, 2015, 35, 1511-1520.	1.7	118
122	CNGB3-Achromatopsia Clinical Trial With CNTF: Diminished Rod Pathway Responses With No Evidence of Improvement in Cone Function. Investigative Ophthalmology and Visual Science, 2015, 56, 1505-1505.	3.3	9
123	ASSESSING PHOTORECEPTOR STRUCTURE AFTER MACULAR HOLE CLOSURE. Retinal Cases and Brief Reports, 2015, 9, 15-20.	0.6	13
124	Correlation of Outer Nuclear Layer Thickness With Cone Density Values in Patients With Retinitis Pigmentosa and Healthy Subjects. Investigative Ophthalmology and Visual Science, 2015, 56, 372-381.	3.3	60
125	En Face Optical Coherence Tomography of Outer Retinal Discontinuity and Fan-Shaped Serous Macular Detachment in Diabetic Macular Edema. JAMA Ophthalmology, 2015, 133, 961.	2.5	2
126	Clinical Insights Into Foveal Morphology in Albinism. Journal of Pediatric Ophthalmology and Strabismus, 2015, 52, 167-172.	0.7	45

#	Article	IF	CITATIONS
127	Single Cell Imaging In Photoreceptor Degenerative Disease. , 2015, , .		0
128	Genotype-Dependent Variability in Residual Cone Structure in Achromatopsia: Toward Developing Metrics for Assessing Cone Health. , 2014, 55, 7303.		67
129	Assessment of Perfused Foveal Microvascular Density and Identification of Nonperfused Capillaries in Healthy and Vasculopathic Eyes. Investigative Ophthalmology and Visual Science, 2014, 55, 8056-8066.	3.3	52
130	Microscopic Inner Retinal Hyper-Reflective Phenotypes in Retinal and Neurologic Disease. , 2014, 55, 4015.		44
131	Author Response: Relationship Between Foveal Cone Specialization and Pit Morphology in Albinism. , 2014, 55, 5923.		2
132	The reliability of parafoveal cone density measurements. British Journal of Ophthalmology, 2014, 98, 1126-1131.	3.9	33
133	A Prospective Longitudinal Study of Retinal Structure and Function in Achromatopsia. , 2014, 55, 5733.		68
134	Cone Structure in Subjects with Known Genetic Relative Risk for AMD. Optometry and Vision Science, 2014, 91, 939-949.	1.2	12
135	Outer Segment Length in Different Best Disease Genotypes—Reply. JAMA Ophthalmology, 2014, 132, 1153.	2.5	7
136	Relationship Between Foveal Cone Specialization and Pit Morphology in Albinism. , 2014, 55, 4186.		119
137	In Vivo Imaging of Human Cone Photoreceptor Inner Segments. , 2014, 55, 4244.		310
138	Retinal Structure and Function in Achromatopsia. Ophthalmology, 2014, 121, 234-245.	5.2	145
139	Author reply. Ophthalmology, 2014, 121, e41.	5.2	Ο
140	Classification of Human Retinal Microaneurysms Using Adaptive Optics Scanning Light Ophthalmoscope Fluorescein Angiography. , 2014, 55, 1299.		110
141	A Lensing Effect of Inner Retinal Cysts on Images of the Photoreceptor Mosaic. Retina, 2014, 34, 421-422.	1.7	13
142	OUTER RETINAL STRUCTURE AFTER CLOSED-GLOBE BLUNT OCULAR TRAUMA. Retina, 2014, 34, 2133-2146.	1.7	35
143	Rapid, Accurate, and Non-Invasive Measurement of Zebrafish Axial Length and Other Eye Dimensions Using SD-OCT Allows Longitudinal Analysis of Myopia and Emmetropization. PLoS ONE, 2014, 9, e110699.	2.5	52
144	Adaptive Optics Retinal Imaging – Clinical Opportunities and Challenges. Current Eye Research, 2013, 38, 709-721.	1.5	76

#	Article	IF	CITATIONS
145	X-linked cone dystrophy and colour vision deficiency arising from a missense mutation in a hybrid L/M cone opsin gene. Vision Research, 2013, 80, 41-50.	1.4	22
146	Adaptation of the central retina for high acuity vision: Cones, the fovea and the avascular zone. Progress in Retinal and Eye Research, 2013, 35, 63-81.	15.5	210
147	Automatic cone photoreceptor segmentation using graph theory and dynamic programming. Biomedical Optics Express, 2013, 4, 924.	2.9	75
148	In vivo imaging of human retinal microvasculature using adaptive optics scanning light ophthalmoscope fluorescein angiography. Biomedical Optics Express, 2013, 4, 1305.	2.9	72
149	Automatic detection of modal spacing (Yellott's ring) in adaptive optics scanning light ophthalmoscope images. Ophthalmic and Physiological Optics, 2013, 33, 540-549.	2.0	42
150	Human Cone Visual Pigment Deletions Spare Sufficient Photoreceptors to Warrant Gene Therapy. Human Gene Therapy, 2013, 24, 993-1006.	2.7	97
151	Relationship Between Foveal Cone Structure and Clinical Measures of Visual Function in Patients With Inherited Retinal Degenerations. , 2013, 54, 5836.		81
152	Outer Retinal Structure in Best Vitelliform Macular Dystrophy. JAMA Ophthalmology, 2013, 131, 1207.	2.5	40
153	SELECTIVE CONE PHOTORECEPTOR INJURY IN ACUTE MACULAR NEURORETINOPATHY. Retina, 2013, 33, 1650-1658.	1.7	41
154	High-Resolution Images of Retinal Structure in Patients with Choroideremia. , 2013, 54, 950.		83
155	RhodopsinF45L Allele Does Not Cause Autosomal Dominant Retinitis Pigmentosa in a Large Caucasian Family. Translational Vision Science and Technology, 2013, 2, 4.	2.2	11
156	Visual Function and Cortical Organization in Carriers of Blue Cone Monochromacy. PLoS ONE, 2013, 8, e57956.	2.5	7
157	The Effect of Cone Opsin Mutations on Retinal Structure and the Integrity of the Photoreceptor Mosaic. , 2012, 53, 8006.		85
158	Subclinical Photoreceptor Disruption in Response to Severe Head Trauma. JAMA Ophthalmology, 2012, 130, 400.	2.4	21
159	Relationship between the Foveal Avascular Zone and Foveal Pit Morphology. , 2012, 53, 1628.		143
160	Repeatability of In Vivo Parafoveal Cone Density and Spacing Measurements. Optometry and Vision Science, 2012, 89, 632-643.	1.2	135
161	Adaptive Optics and Spectral-Domain Optical Coherence Tomography of Human Photoreceptor Structure After Short Pascal Macular Grid and Panretinal Laser Photocoagulation. JAMA Ophthalmology, 2012, 130, 518.	2.4	16
162	Foveal avascular zone and foveal pit formation after preterm birth. British Journal of Ophthalmology, 2012, 96, 961-966.	3.9	110

#	Article	IF	CITATIONS
163	Assessing Retinal Structure in Complete Congenital Stationary Night Blindness and Oguchi Disease. American Journal of Ophthalmology, 2012, 154, 987-1001.e1.	3.3	55
164	Imaging the Photoreceptor Mosaic with Adaptive Optics: Beyond Counting Cones. Advances in Experimental Medicine and Biology, 2012, 723, 451-458.	1.6	16
165	Photoreceptor Structure and Function in Patients with Congenital Achromatopsia. , 2011, 52, 7298.		142
166	Noninvasive imaging of the human rod photoreceptor mosaic using a confocal adaptive optics scanning ophthalmoscope. Biomedical Optics Express, 2011, 2, 1864.	2.9	305
167	Spatial and temporal variation of rod photoreceptor reflectance in the human retina. Biomedical Optics Express, 2011, 2, 2577.	2.9	82
168	Race- and Sex-Related Differences in Retinal Thickness and Foveal Pit Morphology. , 2011, 52, 625.		223
169	Integrity of the Cone Photoreceptor Mosaic in Oligocone Trichromacy. , 2011, 52, 4757.		33
170	Unusual Adaptive Optics Findings in a Patient With Bilateral Maculopathy. JAMA Ophthalmology, 2010, 128, 253.	2.4	10
171	Arrested development: High-resolution imaging of foveal morphology in albinism. Vision Research, 2010, 50, 810-817.	1.4	121
172	Deletion of the X-linked opsin gene array locus control region (LCR) results in disruption of the cone mosaic. Vision Research, 2010, 50, 1989-1999.	1.4	56
173	Color-deficient cone mosaics associated with Xq28 opsin mutations: A stop codon versus gene deletions. Vision Research, 2010, 50, 2396-2402.	1.4	26
174	Retinal imaging using commercial broadband optical coherence tomography. British Journal of Ophthalmology, 2010, 94, 372-376.	3.9	60
175	Adaptive Optics Retinal Imaging: Emerging Clinical Applications. Optometry and Vision Science, 2010, 87, 930-941.	1.2	142
176	Spectral Domain Optical Coherence Tomography and Adaptive Optics: Imaging Photoreceptor Layer Morphology to Interpret Preclinical Phenotypes. Advances in Experimental Medicine and Biology, 2010, 664, 309-316.	1.6	29
177	Assessing the Photoreceptor Mosaic over Drusen Using Adaptive Optics and SD-OCT. Ophthalmic Surgery Lasers and Imaging Retina, 2010, 41, S104-8.	0.7	39
178	Cone photoreceptor mosaic disruption associated with Cys203Arg mutation in the M-cone opsin. Proceedings of the National Academy of Sciences of the United States of America, 2009, 106, 20948-20953.	7.1	65
179	Normality of colour vision in a compound heterozygous female carrying protan and deutan defects. Australasian journal of optometry, The, 2009, 92, 356-361.	1.3	4
180	Variable optical activation of human cone photoreceptors visualized using a short coherence light source. Optics Letters, 2009, 34, 3782.	3.3	61

#	Article	IF	CITATIONS
181	Adaptive optics optical coherence tomography at 120,000 depth scans/s for non-invasive cellular phenotyping of the living human retina. Optics Express, 2009, 17, 19382.	3.4	136
182	Spectral-domain optical coherence tomography and adaptive optics may detect hydroxychloroquine retinal toxicity before symptomatic vision loss. Transactions of the American Ophthalmological Society, 2009, 107, 28-33.	1.4	52
183	In vivo imaging of the photoreceptor mosaic of a rod monochromat. Vision Research, 2008, 48, 2564-2568.	1.4	81
184	Focus on Molecules: The cone opsins. Experimental Eye Research, 2008, 86, 865-866.	2.6	1
185	Adaptive Optics Retinal Imaging. JAMA Ophthalmology, 2008, 126, 857.	2.4	11
186	The L:M cone ratio in males of African descent with normal color vision. Journal of Vision, 2008, 8, 5.	0.3	23
187	Adaptive optics retinal imaging reveals S-cone dystrophy in tritan color-vision deficiency. Journal of the Optical Society of America A: Optics and Image Science, and Vision, 2007, 24, 1438.	1.5	107
188	High-Resolution Retinal Imaging of Cone–Rod Dystrophy. Ophthalmology, 2006, 113, 1014-1019.e1.	5.2	151
189	Retinal Microscotomas Revealed with Adaptive-Optics Microflashes. , 2006, 47, 4160.		64
190	The locus of fixation and the foveal cone mosaic. Journal of Vision, 2005, 5, 3-3.	0.3	144
191	Organization of the Human Trichromatic Cone Mosaic. Journal of Neuroscience, 2005, 25, 9669-9679.	3.6	446
192	Functional photoreceptor loss revealed with adaptive optics: An alternate cause of color blindness. Proceedings of the National Academy of Sciences of the United States of America, 2004, 101, 8461-8466.	7.1	267
193	Variety of genotypes in males diagnosed as dichromatic on a conventional clinical anomaloscope. Visual Neuroscience, 2004, 21, 205-216.	1.0	64
194	Estimates of L:M cone ratio from ERG flicker photometry and genetics. Journal of Vision, 2002, 2, 1-1.	0.3	133
195	Color Perception Is Mediated by a Plastic Neural Mechanism that Is Adjustable in Adults. Neuron, 2002, 35, 783-792.	8.1	260
196	Testing hypotheses about visual pigments underlying deutan color vision. Color Research and Application, 2001, 26, S106-S111.	1.6	2
197	Flicker-photometric electroretinogram estimates of L:M cone photoreceptor ratio in men with photopigment spectra derived from genetics. Journal of the Optical Society of America A: Optics and Image Science, and Vision, 2000, 17, 499.	1.5	82
198	Proteostasis Modulation Prevents Photoreceptor Pathology in Retinal Organoids. SSRN Electronic Journal, 0, , .	0.4	1